ISSN 2250-3153

Improvement of Boss Tower for Single Ball Swaging in Hard Disk Drive

Joompondej Bamrungwongtaree[*], Mongkol Mongkolwongrojn[**]

[*] College of Data Storage Innovation, King Mongkut's Institute of Technology Ladkrabang, Thailand
[**] Mechanical Engineering Department, King Mongkut's Institute of Technology Ladkrabang, Thailand

Abstract- Ball swaging is a material process used to assemble a boss tower and an arm aperture. A swage ball is inserted into the boss tower to swage and couple two components. The swage ball has a larger diameter than an inner diameter of the boss tower, applies a compression force to the inner surface of the boss tower to hold both components together with adequate holding force and without damaging the boss tower. This study proposes a new design of the boss tower by relief ring width optimization. It reduces the arm tip deformation while avoiding HSA resonance and allows similar swaging quality by using single ball. The 3-D FE method was used for analysis. The result analysis and experiment show boss tower deformation very similar. Although the variation of CTQ has been decreased, cleanliness has been improved. Moreover, non-circular arm aperture is able to reduce swage effect.

Index Terms- Ball Swaging, Finite Element, Head Stack Assembly, Spacer Key, Boss Tower

I. INTRODUCTION

In the hard disk drive (HDD) manufacturing process, ball swaging has long been a common process. The process assembles the Head Gimbal Assembly (HGA) base plates with actuator arm called the head stack assembly (HSA). A base plate includes a flange having a top surface and an opposing second surface; and a boss tower having a swage hole and extending from an area where the boss tower meets the top surface of the flange to an end surface of the boss tower. The base plate is a component of a swage coupling assembly that is coupled to a component having an arm aperture as shown in Figure 1. The Figure 2 shows the configuration of the boss tower and the figure 3 shows several types of the boss tower profile which consist of basic components. During the swaging process, the ball is inserted through the boss tower to swage couple the boss tower to the arm aperture that clamped by swage keys. The swage ball applies a compression force to the inner surface of the boss tower, therefore the boss tower expands to hold the second component to the first component with adequate holding force and without damaging the boss tower. The base plate and arm tip deformation cause an effect to many Critical To Quality parameters (CTQ).

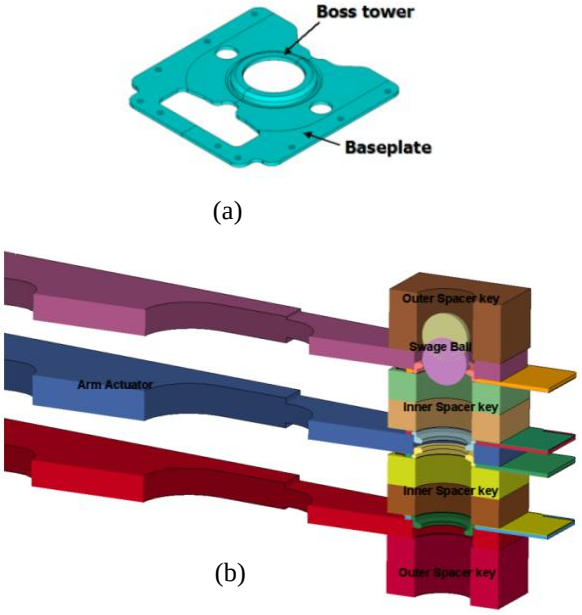

Figure 1: (a) Components of a base plate and (b) the Head Stack Assembly for swaging process

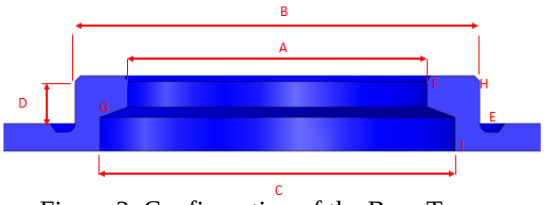

Figure 2: Configuration of the Boss Tower
A = Boss ID, B = Boss OD, C = Backbore Dia., D = Boss Height, E = Relief Ring, F = Top Transition Angles, G = Bottom Transition Angles, H = Back Angles and I = Backbore chamfer

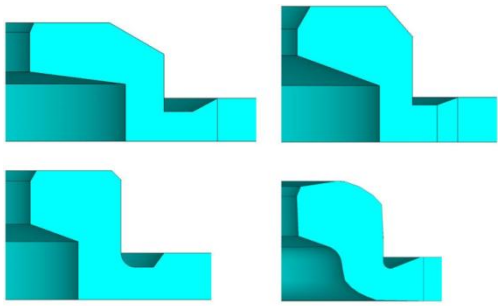

Figure 3: Boss Tower profiles

At present, the hard disk drive (HDD) capacity is dynamically increased while its size becomes slimmer and the read-write head was tightened to move on the media. To reduce the swage effect of the new arm pad and head gimbal designed, all the configuration of the boss tower can be studied to reduce deviation after swaging process. The high deformation has occurred whilst the ball was passing through the boss tower as simply shown in Figure 4. The swaging process results in elastic-plastic deformation of boss tower and actuator arm hole. This deformation can cause disturbance in desired spring characteristic of the suspension on the actuator arm, known as the gramload changes from its design value, and change to desired torque out. Since gramload and torque out are the critical parameters affecting the slider flight height and op-shock performance of hard disk drives, investigating the swaging process that induced base plate and arm deformation, HSA property and torque out change are of main focus. However, it is necessary to clarify the dimension of the boss tower profile to reduce swage effect and for single ball swaging.

The first study, Wadhwa [1] analysed the ball swaging process using an axially symmetric model, and Kittipong [2] numerically verified the deformation of the entire arm and HGA but the accuracy of the simulation has yet to be verified through experimentation. Aoki and Aruga [3] analysis using a three-dimension finite element was based on a symmetrical model for an actuator inner arm and two attached base plates. These studies provide a better understanding of the base plate deformation. In Jian Yang [4]'s analysis using a three-dimension finite element to study gram load changes, helps to understand the relationship between deformation and gram load changes. Some recommendations on having a spacer key to reduce swage effect and resonance analysis by three dimensional finite element analysis model were given [5-8]. Athena Jiao et al. [9] found that the ball size introducing a 15% deformation is preferred for resonance performance.

The aim of this research is to study the effects of the boss tower parameters and to optimize the use of single ball swaging process. The current boss tower will be developed to be used for a single ball in swaging process. The swaging process is investigated by performing explicit dynamic finite element analysis (FEA) using a commercial program ANSYS/LS-Dyna [10]. Initial study is on an arm coupon and validation then move into experiment with ten base plates and six arms in the assembly as a prototype in actual process. The clamping force in a single ball swaging process is considered constant; its velocity remains constant in the top-to-bottom direction.

II. GOVERNING EQUATION

The Figure 4 shows the diagram of the swaging structure. Inherently, the swaging process is a sophisticated problem of metal transformation involving three objects which includes base plate, arm and swage ball that are different in shape and material properties.

Thus, the complete model for the swaging process would be extremely complicated and will be affected by a number of parameters. Many factors are involved which all contribute to the shift of the HSA characteristics. In this paper, the focus is on how to use a one-ball to assemble HSA while maintaining the HSA characteristics. Many parameters relatively were varied.

(a) (b)

Figure 4: (a) Swaging schematic (b) Arm aperture model as thick cylinders

The governing equation of swaging process can be written in equation

$$\frac{\partial \sigma_r}{\partial r} + \frac{\sigma_r - \sigma_\theta}{r} = 0 \tag{1}$$

and

$$\frac{d^4\phi}{dr^4} + \frac{2}{r}\frac{d^3\phi}{dr^3} - \frac{1}{r^2}\frac{d^2\phi}{dr^2} + \frac{1}{r^3}\frac{d\phi}{dr} = 0 \tag{2}$$

Where σ_r and σ_θ are radial and circumferential stresses respectively and ϕ is the Airy's stress function is in the form

$$\phi = \frac{\lambda}{2} r^2 + \beta \log r \tag{3}$$

To simplify the theoretical model and make it is reasonable, the deformation occurring in the swaging process is considered as thick cylinder as shown in Figure 4(b). In absence of body force for this axisymmetric, Lame formula can be used here to calculate the stress generated at different locations [9].

$$\sigma_\theta = \frac{pa^2 - Pb^2}{b^2 - a^2} + \frac{(p-P)a^2b^2}{b^2 - a^2}\frac{1}{r^2} \tag{4}$$

$$\sigma_r = \frac{pa^2 - Pb^2}{b^2 - a^2} - \frac{(p-P)a^2b^2}{b^2 - a^2}\frac{1}{r^2} \tag{5}$$

The displacement can be derived using the formula below.

$$u_r = \frac{1}{E}\left[\frac{(1-\upsilon)(pa^2 - Pb^2)}{b^2 - a^2} r + \frac{(1+\upsilon)a^2b^2(p-P)}{b^2 - a^2} r\right] \tag{6}$$

With Tresca rules applied [9], then further relationship can be derived, material will begin to yield when τ_{max}, the maximum shear stress, is equal to τ_y the yield stress. Since σ_θ and σ_r are principal stresses, yielding will begin when

$$\tau_{\max} = \frac{\sigma_\theta - \sigma_r}{2} = \tau_y \tag{7}$$

Now define a radius r_p so that region $a \le r \le r_p$ is in the plastic region and $r_p \le r \le b$ is in the elastic region then obtain

$$\sigma_r = -2\tau_y \log\frac{r_p}{r} - p_{r_p} \; ; a \le r \le r_p \tag{8}$$

The ball size will affect the inner pressure applied to the boss tower and then further engage to an arm hole. The relationship between ball size and the inner pressure force is as well as the degree of plastic deformation of base plate and boss tower. In the actual swaging process, the base plate's boss tower is more complicated than in the simulation. Thus, the finite element analysis will be used to study for the single ball swaging to approach this behaviour.

III. SWAGING NUMERICAL MODEL

The finite element simulation of a single ball swaging process was performed with the commercial software package. The explicit dynamics simulation, the equilibrium equations in dynamic analysis can be written in the form

$$[M]\left[\ddot{u}^{(i)}\right] = \left[F^{(i)}\right] - \left[I^{(i)}\right] \tag{9}$$

where [*M*] is mass matrix, *F* is the vector of externally applied load and *I* is the vector of inertia forces. The mathematically equilibrium relation is a system of linear differential equations of second order. The solution can be obtained by finite difference expression to approximate the accelerations and velocities in terms of displacement which can be written as

$$\ddot{u}^{(i)} = \frac{1}{\Delta t^2}\left(u^{(i+1)} - 2u^{(i)} + u^{(i-1)}\right) \tag{10}$$

The error of calculation depends on stable increment of time as the relation is shown below

$$\Delta t_{stable} = \min\left(\frac{L_c}{c}\right) \tag{11}$$

where L_c is limited element edge length and c is velocity of longitudinal wave for an element is in the form

$$c = \sqrt{\frac{\lambda + 2\mu}{\rho}} \tag{12}$$

λ and μ is Lame' constants can be written in terms of young's modulus and passion ratio as follows

$$\lambda = \frac{\upsilon E}{(1+\upsilon)(1-2\upsilon)} \tag{13}$$

$$\mu = \frac{E}{2(1+\upsilon)} \tag{14}$$

The stable time expression mentioned for only one element in practically the LS-DYNA solver automatically calculates the minimum time step for each element based on its characteristic length and density. The smallest of these element time steps is called the critical time step. The actual time step used during solution is the product of the current critical time step and a stability factor (usually 0.90). As elements distort during the analysis, their time steps are recalculated. However, an element's time step is calculated based on its material properties (E,υ,ρ) and characteristic length. The equation can be rearranged to find the required density of each element for a desired time step size. By adding the corresponding mass to these elements, the solution time will be reduced. This procedure is known as mass scaling and not recommended. In this paper, mass was not added to speed up run. A three-dimensional (3-D) and a cross-sectional view of the finite element (FE) model used for swaging process of actuator arms are shown in Figure 5 and 6.

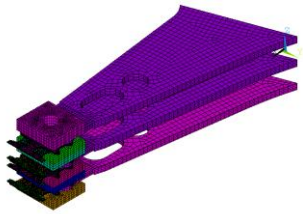

Figure 5: Four base plate and three arms in the assembly for swaging simulation

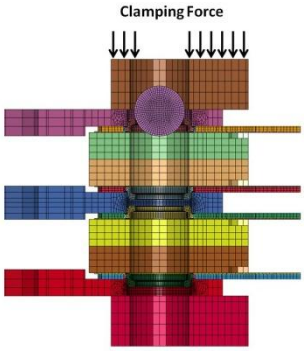

Figure 6: Cross-sectional view of four base plates and three arms in the assembly for swaging simulation

The swage torque out after the ball is driven through the boss tower the base plate and attached suspension was securely fastened to the actuator arm pad. The equation of swage torque can be derived from

$$T = rF \tag{15}$$

Where

$$F = \mu N \tag{16}$$

And now substitution eq. (16) into eq. (15) got

$$T = r\mu \int_0^{2\pi} P \frac{rL}{N_e} d\theta \tag{17}$$

Simplify the eq. (17) obtain

$$T = \mu PA\frac{D}{2N_e} \tag{18}$$

where T is HGA torque out, μ is coefficient of friction, P is contact pressure, D is a diameter of swage hole, and N_e is the number of engaged element. Practically, an average pressure and contact area substitution in (18) to obtain HGA torque out. However, current process has standard swage and micro-swage; the swage torque out relation of both can start from (15). For standard swaging,

$$T_s = r_s F_s \tag{19}$$

Where $F_s = 2\pi r_s \mu_s$ then

$$T_s = \mu_s 2\pi r_s^2 \tag{20}$$

Solving for μ

$$\mu = \frac{T_s}{2\pi r_s^2} \tag{21}$$

As for micro-swage start from eq. (15)

$$T_{ms} = r_{ms} F_{ms} \tag{22}$$

Solving for μ

$$\mu = \frac{T_{ms}}{2\pi r_{ms}^2} \tag{23}$$

From Eq. (21) and (23) obtain

$$\frac{T_s}{2\pi r_s^2} = \frac{T_{ms}}{2\pi r_{ms}^2} \tag{24}$$

Thus

$$T_s = \frac{r_s^2}{r_{ms}^2} T_{ms} \tag{25}$$

Equation (25) is theoretical micro-swage flange effect comparison where T_s is standard HGA torque out, T_{ms} is micro-swage HGA torque out, r_s is radius of standard swage, r_{ms} is radius of micro-swage. In this analysis, a nonlinear explicit dynamics analysis is performed. The swaged part of the base plate undergoes plastic deformation. Nonlinear material properties are considered. To save time consumption, the model is presented with three actuator arm tip, four base plates with part of hinges, four swage keys, and one swage ball. The inner spacer key was separated to two part of assembly for specific analysis, as shown in Figure 6. As for the experiment, six arms with ten headers are used.

IV. BOUNDARY CONDITIONS AND CONTACT SURFACES

During the swaging process, the constant clamping force at the outer key parts during swaging is constant and the arms are separated from each other by the spacer keys. In the FE model, the clamping pressure is applied as forces via force load curve. In other words, the swage keys, which are employed to simulate the clamping boundary at the arm contact condition, are partial modelled as rigid bodies and does not include spacer key's tail while the other components including actuator arm tip, base plates and hinges are deformable parts. The simulation uses the same load curve for ball speed for each heads and swage ball; and is forced to move in Z direction only according to its load curve. The boss tower of the base plate is plastically deformed and joined to the arm. The contact surface between the ball and swaging boss, between the base plate and the arm, and the one between swaging boss and the clamp are taken into account in analysing the boss arm force. The friction coefficients for each contact surface are divided into two groups, contact surface of assembly and part-to-part contact. The base plate, hinge and the suspension are made of stainless steel while the arm is made of aluminum. The swaging ball is made of stainless steel with hardened coating. Thus, the ball is simulated as a rigid body. The material models defined in the analysis are bilinear isotropic material and bi-linear kinematics hardening. The properties of the materials used in the simulation are listed in Table 1. The interesting area will be defined as component name to recall in post processor.

All the elements used in the analysis are eight-nodes brick elements. To further reduce the computing time, the model consists of both rigid bodies and deformable bodies. The actuator arm hole and the base plate's boss tower are prepared and that the finer meshes are only required in the vicinity of the contact areas and the elements are coarser in the areas farther away.

Table 1: Material properties for finite element analysis

Material Properties	Type of Materials	
	Stainless steel	Aluminum
Elastic modulus, E (MPa)	190,000	71,016
Yield stress, Y (MPa)	206	275
Poisson ratio	0.32	0.33
Mass density (kg/m^3)	7,889	2,700

V. FINITE ELEMENT MODEL VALIDATION

The boss tower and arm tip deformation results from FEA simulations for inner and outer arms are evaluated from the displacements value that measured from specific nodes compared to the reference plane. For all simulated cases, the results have tendency to value from experimental data with strictly control the incoming part. However, the focus is on the effect of the boss tower to maintain the HSA characteristics with single ball which accompany with cost saving, there are some offset that must be controlled. These differences could be from some other effects that were not considered in the present analysis for sample swage shuttle. The illustration of boss tower deformation from swaging process is shown in Figure 7 and 8.

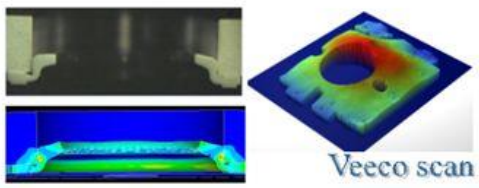

(a)

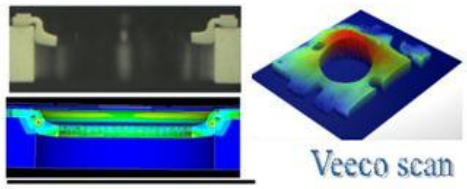

(b)

Figure 7: (a) DN Facing head (b) UP Facing head comparison boss tower X-section deformation and Veeco scan

(a)

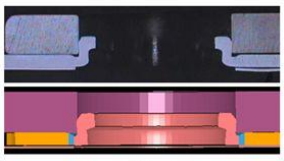

(b)

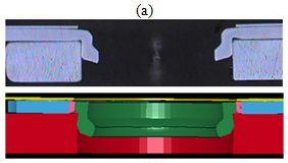

(c)

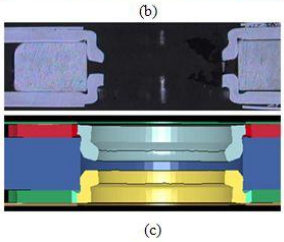

Figure 8: (a) Head #3 (b) Head #1 and 2 (c) Head #0 comparison boss tower X-section deformation

VI. RESULTS AND DISCUSSIONS

In this study, the behaviors and characteristics of the base plate's boss tower profile after a completed swaging process are studied. Table 2 shows comparison between simulation and experimental results. This paper presented the results of screening parameters on process optimization of key parameters for single ball swaging. The optimal parameter setting yield the optimum performance with three parameters after sereening from nineteen parameters. In this case, these parameters are main effect of the parameter variation. The main parameters that affected HSA characteristics are the base plate relief ring width both DN and UP Tab as shown in Figure 9.

Table 2: Simulation and experimental results

Parameters		Tip Height (inch)		Tip Pitch (degree)	
		FEA result	Actual data	FEA result	Actual data
Head 0	Outer arm	-0.00123	-0.00102	-0.572	-0.672
Head 1	Inner arm	0.00031	0.00027	0.473	0.537
Head 2	Inner arm	-0.0006	-0.0009	-0.520	-0.517
Head 3	Outer arm	0.00122	0.00118	0.437	0.543

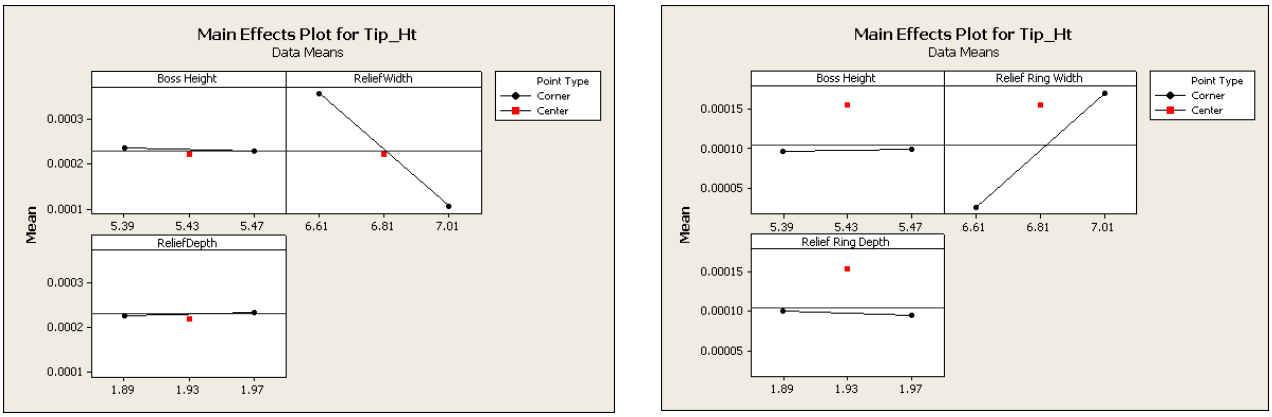

Figure 9: Main effect plot for (a) DN Tab, Tip_Ht (b) UP Tab, Tip_Ht

After the effects of three parameters i.e boss height, relief width and relief depth were screened from nineteen parameters, the result from the simulation will be used for optimal factor setting. The optimum parameter is shown in the Figure 10. The other two parameters were fixed at the same condition to find the proper relief ring width. Obviously from experiment, larger relief ring width provides torque out a bit higher both two tabs for outer arm and comparable with the middle arm. UP tab should be small relief ring width. On the other hand, DN tab should be large.

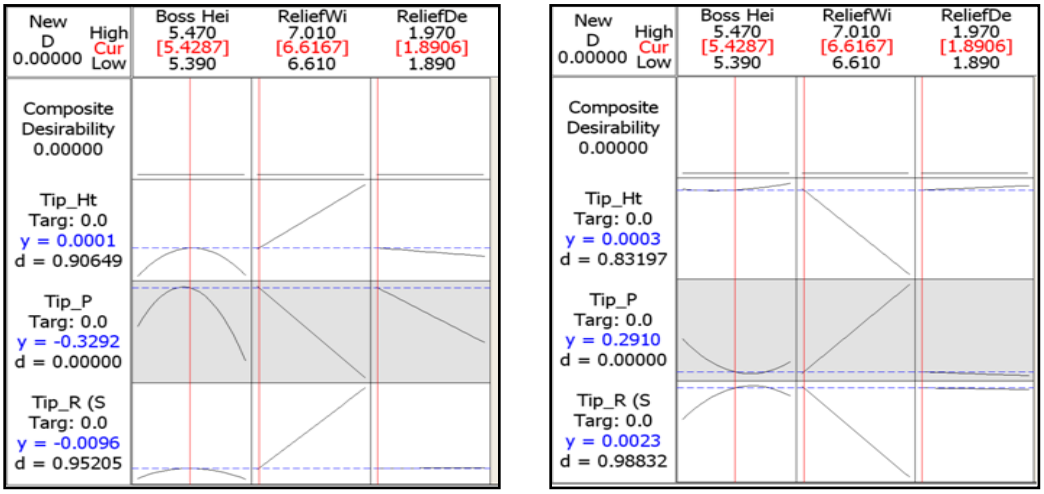

(a) (b)

Figure 10: Optimization (a) UP Tab (b) DN Tab

From this analysis, it leads to new design of the boss tower by relief ring width optimization. A relief ring is not identical width which distance A is more than that B as shown in Figure 11. Figure 12 shows cross section of the optimal relief ring width. Moreover, this design is able to avoid HSA resonance (Nyquist frequency of using 256 servo sectors) similar to using loctite HGA to arm. The experimental results reveal that the frequency shifted from 11kHz to 12kHz. The actual part of HGA torque out, actual cross section, the actual HSA for ten headers are studied and tested and those results reveal that arm tip deformation is reduced as shown in Figure 13. The HSA ten header with single ball swaging was tested the resonance of FRF, the result are acceptable and shift the 11.5kHz to lower frequency to avoid resonance. Also found that the single ball swaging process for ten headers approach to KPIV chart model. The effects of swage shuttle, spacer key land on swaging process will be used as STX DFM.

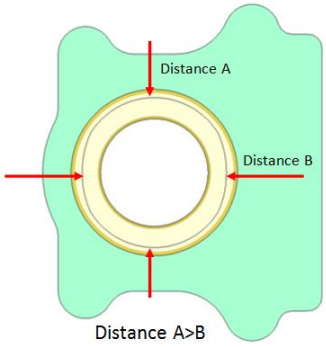

Figure 11: Optimal relief ring width

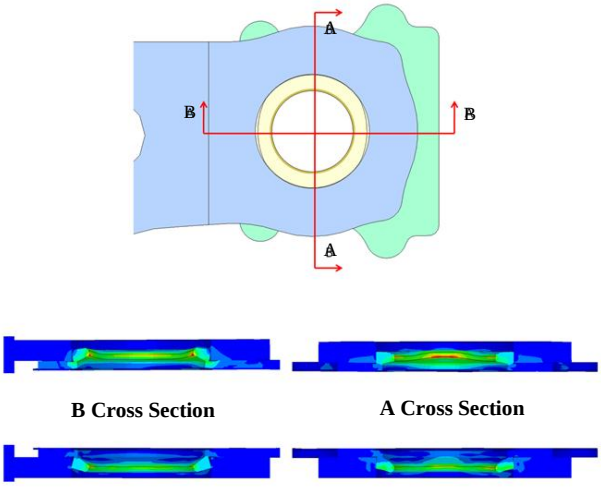

Figure 12: Cross section of the optimal relief ring width

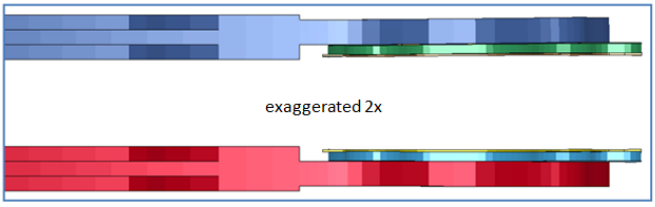

(a)

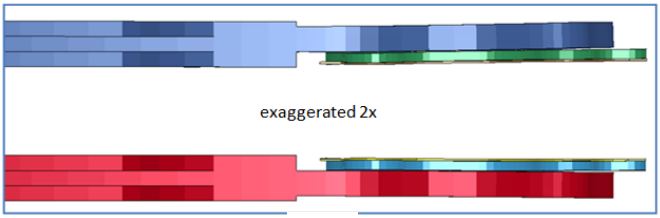

(b)

Figure 13: Relief ring width (a) Optimized cause less deformation both TAB UP and DN (b) Non-Optimized

VII. CONCLUSION

In this paper, the behaviors and characteristics of the base plate's boss tower profile were studied. The analysis reveals that the relief ring width should be a main focus when using single ball in swaging process. The analysis leads to a new design of the boss tower by combination of optimal relief ring width together. Figure 11 illustrates a schematic diagram of a perimeter of relief ring. In particular, Figure 12 and 13 illustrate how the perimeter varies from a minimum compression force to a maximum compression force. The experimental result also shows that the arm thickness is not related to HGA torque out. Still, the impact to arm tip deformation leads to resonance frequency. The new design of boss tower is able to apply with thin arm for reduction of the arm tip deformation. From analysis, the relief ring depth excessive results in flange effect. A small top transition angle can reduce the boss tower deformation. The very low bottom transition angle results in swage push out defect. The backbore diameter is used for boss tower hinging. Although relief ring is mainly a potential impact to HSA quality, for a single ball swaging, not only relief ring is improved, in actual process some parameters also are slightly adjusted to keep HSA characteristics CTQ and swage push out is decreased; thus a contact angle is recommended. Back bore chamfer is required to reduce suspension weight, right angle can be ignored for back bore. When re-work is considered, there is no impact to the installed head due the same ball size is used and just passed through. However, HSA lower header has lower impact to HSA characteristics because long distance has more chance to face swage damage if ball speed is increased. The dimension of spacer key land should be controlled to ensure that other defect will not occurred during swaging process. From eq. 25, with STX boss tower the standard swage has HGA torque out approximately two times of micro-swage.

ACKNOWLEDGMENT

This study is supported by Cooperate Project between National Electronics and Computer Technology Center (NECTEC) and Seagate Technology (Thailand) via Industry/University Cooperative Research Center (I/UCRC) in HDD Component, King Mongkut's Institute of Technology Ladkrabang.

REFERENCES

[1] S.K. Wadhwa, "Material Compatibility and Some Understanding of the Ball Swaging Process," *IEEE Transactions on Magnetics*, Vol. 32, No. 3, 1996, pp. 1837-1842.
[2] E. Kittipong, C. Surachate, K. Thoatsanope, "Effects of Swaging Process Parameters on Specimen Deformation," *Eighth Asian Symposium on Visualization*, Chiangmai, Thailand, 2005, pp.50.1-50.7.
[3] K. Aoki and K. Aruga, "Numerical Ball Swaging Analysis of Head Arm for Hard Disk Drives," *Microsyst. Technol*, Vol. 13, 2007, pp. 943-949.
[4] L. Chen-Chi, Y. Jian, and Ti. Shahab, "Finite Element Simulation of Ball Swaging Process of Jointing HGA With Actuator Arm and Gram Load Calculation," *ASME Information Storage and Processing Systems Conference*. 2007. Santa Clara, CA.
[5] B. Joompon, "Effect of the Spacer Key on Swage Push out," *International Conference of Business and Industrial Research*, Bangkok, Thailand, 17-18 March 2010.Bangkok, Thailand.
[6] B. Joompon, "Effect of the Spacer Key to HAS," *3rd International Conference on Data Storage Technology*, Bangkok, Thailand, 2010, pp.131-134
[7] B. Joompon, "Study of Outer Key to Reduce Outer Arm Swage Effect," *Joint International Conference On Information & Communication Technology Electronic and Electrical Engineering, Luangprabang*, Lao PRD, 2010, pp.16-19
[8] B. Joomponladej, "A Development of modeling for Resonance Analysis," 4th *International Conference on Data Storage Technology*, Bangkok, Thailand, 2011, pp.108-111
[9] A. Jiao, Z. Liu, L. Pan, M. Ying, "Swaging Force Control in Drive Resonance Response," *IEEE Trans. Magnetic Recording Conference*, Singapore, 2009, pp. BS04
[10] Livermore Software Technol. Corp. *LS-Dyna Theory Manual*, Livermore, CA, 2006.

AUTHORS

First Author – Joompondej Bamrungwongtaree, M.Eng, King Mongkut's Institute of Technology Ladkrabang , joompondej.bamrungwongtaree@seagate.com.

Second Author – Mongkol Mongkolwongrojn, Ph.D (Mechanical Engineering), King Mongkut's Institute of Technology Ladkrabang, kmmongko@kmitl.ac.th

Correspondence Author – Pattaraweerin Woraratsoontorn, oaw2520@hotmail.com, jomeb@hotmail.com, (66)96472455.